Numerical analysis of vortex motion on Josephson structures

doi: 10.1063/1.1663917

Numerical analysis of vortex motion on Josephson structures

Koji Nakajima and Yutaka Onodera

Research Institute of Electrical Communication, Tohoku University, Sendai, Japan

Tadao Nakamura and Risaburo Sato

Department of Electrical Communications, Faculty of Engineering, Tohoku University, Sendai, Japan
(Received 1 April 1974)

The one-dimensional and two-dimensional sine-Gordon equations with dimensionless loss factors and unitless normalized bias are numerically calculated by computer. The results are presented for accelerations, velocities, collisions, coupled states, and two-dimensional propagation of solitons.

INTRODUCTION

There has been much interest in the Josephson transmission lines because of their potential applications in electronics.[1-4] The Josephson line without losses and bias current can be analyzed with the sine-Gordon equation (SGE).[1,3-7] The exact soliton solutions of the equation have been given[7-13] so that the behaviors of solitons which correspond to the flux quanta in the case of the Josephson line can be known in detail.[3-6,14] Perring and Skyrme have studied interacting mesons by means of the SGE.[8] The propagation of flux quanta on a Josephson line which include the effects of loss and a distributed bias source has been investigated by Scott[4,5] and Johnson.[15] They showed that an arbitary number of flux quanta propagate as a wave of permanent profile, but it appeared that these pulses might exhibit a mode of instability in which individual fluxons detatch themselves from the trailing edge.

On the other hand, the one-dimensional mechanical analogs of the Josephson line have been constructed by Scott[3,4,6] and other authors.[16] These analogs are helpful in understanding the various behaviors of the flux quanta in the Josephson line vividly. However, it is difficult to treat the analogs in terms of high accuracy and the wide range of parameters needed. As described in this paper, the two-dimensional mechanical analog of the Josephson line is designable, but it is difficult to construct the analog to operate correctly.

We have numerically calculated the behavior of solitons on the one-dimensional and the two-dimensional[1,6,12] transmission lines whose models include a unitless normalized bias and dimensionless loss factors. It is purpose of this paper to describe the behavior of solitons under acceleration, the velocity in the stationary state, the propagation modes of solitons, and the collisions of solitons propagating in opposite directions on the one-dimensional transmission line. And finally, we describe the configuration of the soliton propagation on the two-dimensional transmission lines.

EQUATIONS OF THE JOSEPHSON LINE AND THEIR APPROXIMATIONS

The Josephson transmission line, which includes the effects of losses associated with the flow of normal electrons parallel to the junction in addition to losses associated with normal electrons tunnelling through the junction and a distributed bias current source, is described by the following normalized nonlinear partial differential equation[4,15]:

$$\kappa \frac{\partial^3\phi}{\partial x^2 \partial t} + \frac{\partial^2\phi}{\partial x^2} - \frac{\partial^2\phi}{\partial t^2} - \Gamma \frac{\partial\phi}{\partial t} = \sin\phi - \gamma, \tag{1}$$

where $\kappa = L(2\pi J_c/\Phi_0 C)^{1/2}/r$; $\Gamma = g(\Phi_0/2\pi J_c C)^{1/2}$; $\gamma = j_B/J_c$; $\Phi_0 = h/2e$ is the flux quantum; J_c is a constant giving the maximum Josephson current per unit length; L, C, r, g, and j_B are the series inductance, the shunt capacitance, the series resistance, the shunt conductance, and the distributed bias current source per unit length, respectively; and where distances are measured in units of $\lambda_J = (\Phi_0/2\pi L J_c)^{1/2}$ and time in units of $\tau_J = (\Phi_0 C/2\pi J_c)^{1/2}$. Its equivalent circuit is shown in Fig. 1.[4] Equation (1) also describes the mechanical line which we have constructed and reported.[16] If the effects of the series resistance can be neglected, Eq. (1) is written in the form

$$\frac{\partial^2\phi}{\partial x^2} - \frac{\partial^2\phi}{\partial t^2} - \Gamma \frac{\partial\phi}{\partial t} = \sin\phi - \gamma. \tag{2}$$

If one considers the width of the Josephson line, which is smaller than $2\lambda_J$ because of the uniformity of the bias current, Eq. (2) becomes

$$\frac{\partial^2\phi}{\partial x^2} + \frac{\partial^2\phi}{\partial y^2} - \frac{\partial^2\phi}{\partial t^2} - \Gamma \frac{\partial\phi}{\partial t} = \sin\phi - \gamma. \tag{3}$$

Some exact soliton solutions of the sine-Gordon equations, $\nabla^2\phi - \partial^2\phi/\partial t^2 = \sin\phi$, have been obtained,[3-13] but exact solutions of Eqs. (1)—(3) cannot be obtained analytically. To investigate the behavior of solitons given by Eqs. (1)—(3), we use the following finite-difference equations for approximations of Eqs. (1)—(3):

$$\frac{\kappa(I+1)[\phi(N,I+1) - \phi(N,I)] - \kappa(I)[\phi(N,I) - \phi(N,I-1)]}{\Delta x^2 \Delta t}$$

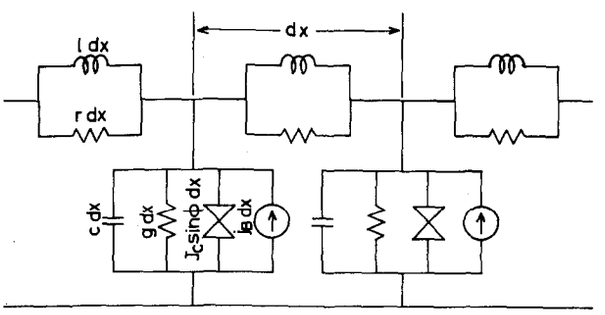

FIG. 1. Equivalent circuit of the Josephson transmission line with bias and losses.

$$-\frac{\kappa(I+1)[\phi(N-1,I+1)-\phi(N-1,I)]}{\Delta x^2\Delta t}$$

$$+\frac{-\kappa(I)[\phi(N-1,I)-\phi(N-1,I-1)]}{\Delta x^2\Delta t}$$

$$+\frac{A(I+1)[\phi(N,I+1)-\phi(N,I)]-A(I)[\phi(N,I)-\phi(N,I-1)]}{\Delta x^2}$$

$$-\frac{B(I)[\phi(N+1,I)-\phi(N,I)]-B(I)[\phi(N,I)-\phi(N-1,I)]}{\Delta t^2}$$

$$-\Gamma(I)\frac{\phi(N,I)-\phi(N-1,I)}{\Delta t}$$

$$=C(I)\{\sin[\phi(N,I)]-\gamma(I)\}, \tag{4}$$

$$\frac{A(I+1)[\phi(N,I+1)-\phi(N,I)]-A(I)[\phi(N,I)-\phi(N,I-1)]}{\Delta x^2}$$

$$-\frac{B(I)[\phi(N+1,I)-\phi(N,I)]-B(I)[\phi(N,I)-\phi(N-1,I)]}{\Delta t^2}$$

$$-\Gamma(I)\frac{\phi(N,I)-\phi(N-1,I)}{\Delta t}$$

$$=C(I)\{\sin[\phi(N,I)]-\gamma(I)\}, \tag{5}$$

where N denotes a point on the t axis, I denotes a point on the x axis, $A(I)=B(I)=C(I)=1.0$, $\kappa(I)=\kappa$, $\Gamma(I)=\Gamma$, $\gamma(I)=\gamma$, Δx is the small increment of space in the x direction, and Δt is the small increment of time. We study numerically the behavior of solitons by using Eqs. (4) and (5) on a digital computer. The exact solutions of the equation

$$\frac{\partial^2\phi}{\partial x^2}=\sin\phi$$

are used to start the calculations of Eqs. (4) and (5). For the boundary conditions, we consider the condition

$$\frac{\partial\phi}{\partial x}=0$$

at all boundaries.

COMPUTER SIMULATIONS OF THE MOTION OF SOLITONS

The small increment of space Δx is selected to be 1.0 in order to be compared with the results of the mechanical analog which we have constructed.[16] But in order to investigate the accelerated solitons, Δx is selected to be 0.1, and 0.4 with respect to the two-dimensional SGE.

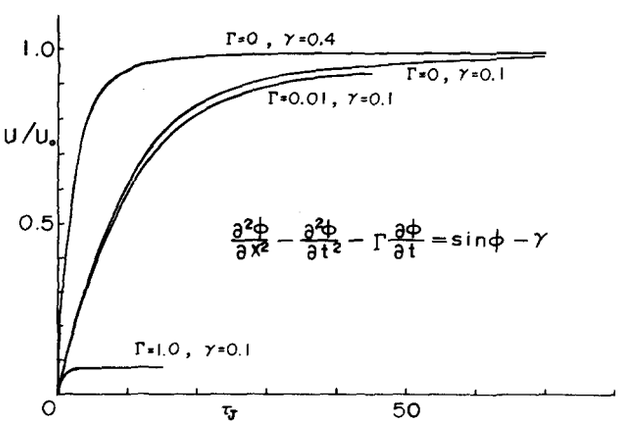

FIG. 2. Normalized velocity u/u_0 of the soliton being accelerated as a function of the time measured in units of τ_J for various values of the dimensionless parameter Γ and γ.

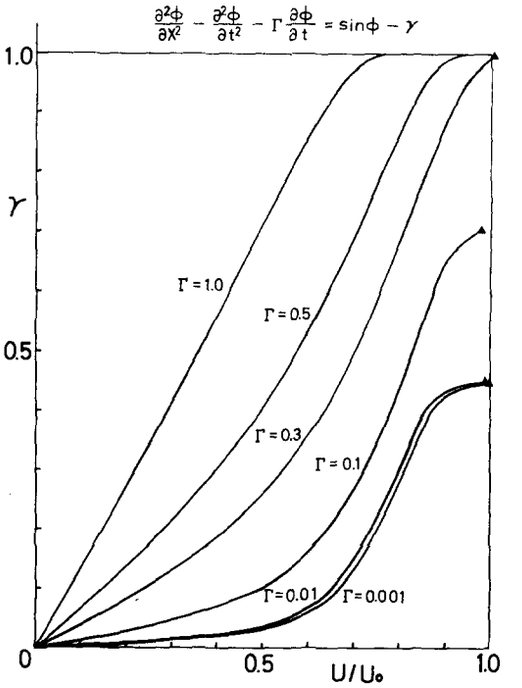

FIG. 3. Normalized velocity u/u_0 of a soliton as a function of the dimensionless parameter γ for various values of the dimensionless parameter Γ. Here $\kappa=0$.

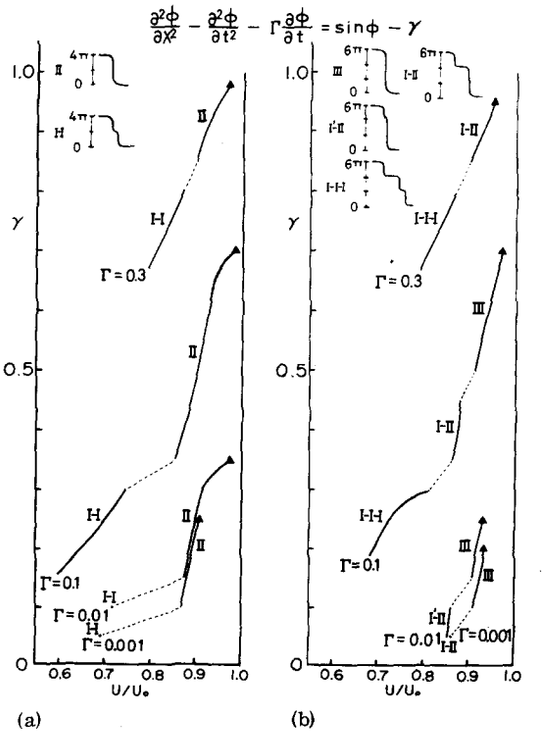

FIG. 4. Normalized velocity u/u_0 of a pulse containing two and three solitons each as a function of the dimensionless parameter γ for various values of the dimensionless parameter Γ. Here $\kappa=0$.

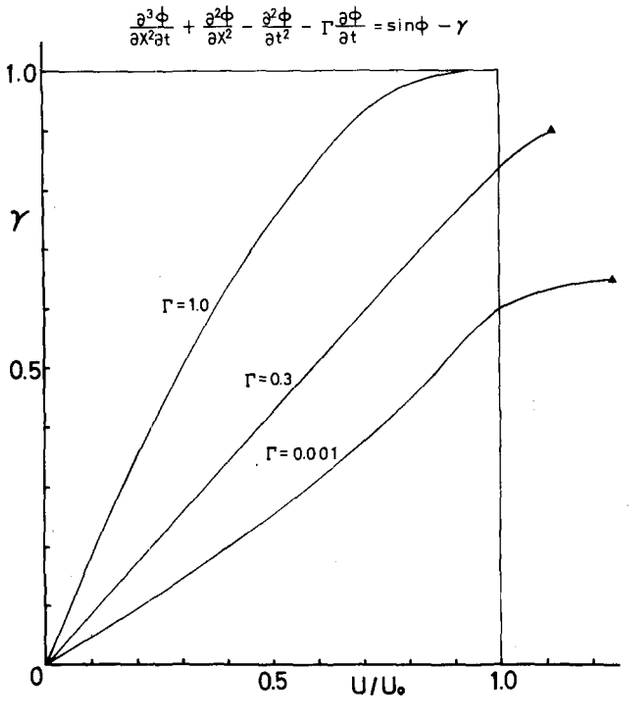

FIG. 5. Normalized velocity u/u_0 of a soliton as a function of the dimensionless parameter γ for various values of the dimensionless parameter Γ. Here $\kappa = 1.0$.

Figure 2 shows the normalized velocity u/u_0 of the soliton being accelerated which is calculated by using Eq. (5) as a function of the time measured in units of τ_J for various values of the dimensionless parameters Γ and γ. Here u_0 is the limiting velocity of the solitons. By decreasing the effects of loss, it takes a long time until the soliton velocity is steady, but the value of steady velocity is higher. If all the effects of the losses are neglected and $\gamma \neq 0$, the soliton velocity saturates in a relatively short time. u is defined as the velocity of the soliton at the point when $\phi = \pi$. When the loss ≈ 0 and $\gamma \approx 1.0$, the creation of many pairs of solitons with opposite screw senses following the transmitting soliton is brought about. Consequently, bunched n solitons and $n-1$ solitons propagate down in opposite directions with $u \approx u_0$. The number of n increases as time increases. The same phenomena are brought about when γ is applied suddenly, if $\gamma < 1.0$.

The normalized velocity u/u_0 of a pulse containing one, two, and three solitons, which are calculated by using Eq. (5), are shown in Figs. 3, 4(a), and 4(b), respectively, as a function of the dimensionless parameter γ for various values of the dimensionless parameter Γ. These results correspond to those of the mechanical analog.[16] For the points denoted by the solid triangle, where the pulse approaches the limiting velocity in these figures, many pairs of solitons with opposite screw senses are created following the transmitting pulse. In the region denoted by II in Fig. 4, two solitons which are bunched rather closely together propagate down. In region I-I, a pulse containing two solitons bunched together shows a tendency to split up into two pulses containing one soliton each. But the two solitons are not completely separated; the space between the two solitons are kept at a constant distance depending upon the values of Γ and γ. In region III, three solitons bunched together propagate down. In region I-II, three transmitting solitons bunched together split up into two solitons bunched togehter and one soliton which becomes detached from the trailing pulse edge. The detached soliton is left behind the two solitons bunched together because of the difference of their velocities. In region I'-II, three transmitting solitons bunched together split up into two solitons bunched together and one soliton which is not completely detached from trailing pulse edge. In region I-I-I, a transmitting pulse containing three solitons bunched together splits up into three pulses containing one soliton each. The velocity of a pulse containing bunched solitons increases with an increase in the number of the bunched solitons for the same values of Γ and γ. The transmitting coupled solitons are stable on the line corresponding to the appropriate γ values, in spite of the repulsive forces among solitons with same screw senses.

The normalized velocity u/u_0 of one soliton, which is calculated using Eq. (4), is shown in Fig. 5 as a function of the dimensionless parameter γ for various values of the dimensionless parameter Γ. κ is estimated to be very large to clarify the effects of the $\partial^3\phi/\partial x^2\,\partial t$ term in Eq. (1). It can be seen from Figs. 3 and 5 that the soliton velocity with $\partial^3\phi/\partial x^2\partial t$ is lower than that given by Eq. (5) for the same values of γ and Γ. The reason for the lower velocity is that $\partial^3\phi/\partial x^2\partial t$ represents the effects of series resistance. But the soliton velocity given by Eq. (4) can be faster than the limiting velocity given by Eq. (5); moreover, the soliton with $u/u_0 > 1.0$ is stable. In this case the creation of many pairs of solitons with opposite screw senses following the transmitting soliton is

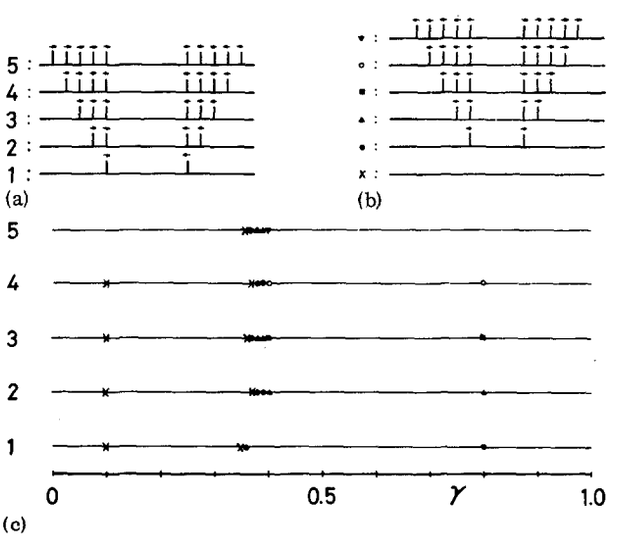

FIG. 6. Collisions of solitons with opposite screw senses and opposite propagating directions as a function of the dimensionless parameter γ for the values of $\Gamma = 0.3$ and $\kappa = 0$. Five kinds of states of solitons before collision are denoted by 1, 2, 3, 4, and 5 in (a). The states of solitons after collisions are denoted by symbols shown in (b). The spaces among the center of the solitons of same screw sense are $10.0\lambda_J$. ↑ denotes a soliton propagating in the direction of the arrow.

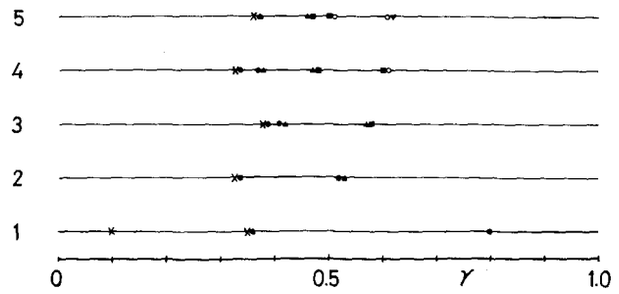

FIG. 7. Collisions of solitons with opposite screw sense and opposite propagating directions as a function of the dimensionless parameter γ for the values of $\Gamma = 0.3$ and $\kappa = 0$. The spaces among the center of the solitons of same screw sense are $5.0\lambda_J$.

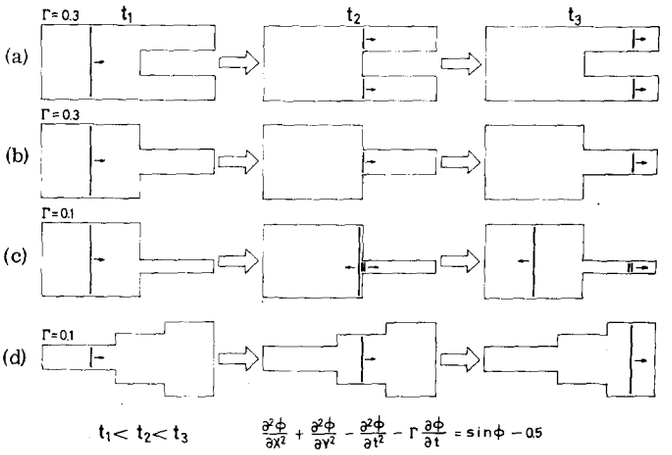

FIG. 8. Propagation modes of a vortex line transmitting on the representative two-dimensional Josephson lines. | → denotes a vortex line propagating in the direction of the arrow.

brought about at $u/u_0 > 1.0$. We have tried the numerical calculations for the value of $\kappa = 0.01$ with respect to the behavior for the cases of one, two, and three transmitting solitons. These results are very similar to the results given by Eq. (5).

The numerical results, which are calculated using Eq. (5) with the value of $\Gamma = 0.3$, for the collisions of solitons with opposite screw senses and opposite propagating directions are shown in Figs. 6 and 7. In Fig. 6, the spaces among the center of the solitons of same screw sense are $10.0\lambda_J$. In Fig. 7, the corresponding spaces are $5.0\lambda_J$. Figure 6(a) shows five kinds of states of solitons before collisions, and the symbols shown in Fig. 6(b) denote the states of solitons after collisions. The numerical results of the collisions of solitons are given in Figs. 6(c) and 7, corresponding to the denoted numbers in Fig. 6(a) as a function of the dimensionless parameter γ. These results can be compared with those of the mechanical analog[16] so that these are reasonable in terms of the effects of the loss, the kinetic energy, and the number and mutual phase relations of colliding solitons. In general, the number of solitons which pass through each other increases with an increase in the value of γ.

The above calculations with respect to the velocities of pulses containing one, two, and three solitons each, and with respect to the collisions of solitons, are also carried out for the value of $\Delta x = 0.4$ and give results which are qualitatively similar to the results of $\Delta x = 1.0$.

We have numerically calculated some results for solitons transmitting on two-dimensional lines of various shapes. Figure 8 shows how the vortex propagates on the representative lines. These results are easily understood by assuming the two-dimensional mechanical analog of SGE shown in Fig. 9. The mechanical analog consists of pulleys, which are fastened bobs, and are connected with elastic rubber belts to each other. Figure 8(a) shows that one transmitting vortex line can be divided into two vortex lines at the fork with two branches. Figure 8(b) shows that the width of the transmitting vortex line becomes shorter and that the vortex line propagates along the contracted Josephson line. But depending upon Γ, γ, and the ratio between the width of the wider part and that of the narrower part of the Josephson line, the vortex line may be reflected at the edge of the wider part of the Josephson line, and consequently two vortex lines propagate along the narrower part of the Josephson line as shown in Fig. 8(c). Figure 8(d) shows that the length of the transmitting vortex line becomes longer and that the vortex line propagates along the wider part of the Josephson line. But depending upon Γ, γ, and the ratio between the width of the narrower part and that of the wider part of the Josephson line, there is another case in which the vortex line cannot enter the wider part and halts at the boundary.

CONCLUSIONS

The one-dimensional and two-dimensional sine-Gordon equations with dimensionless loss factors and unitless normalized bias were numerically calculated by the digital computer NEAC 2200/700 in the computer center of Tohoku University. These calculations are carried out on accelerated solitons, on the velocity of pulses containing one, two, and three solitons each in stationary states, on the state of colliding solitons, and on propa-

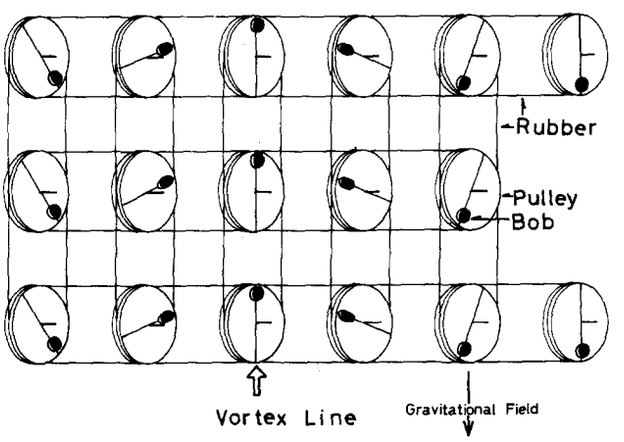

FIG. 9. Mechanical analog of the two-dimensional SGE. This consists of pulleys, which are fastened bobs, connected by rubber belts to each other.

gation states of one soliton given by the two-dimensional SGE.

The results obtained in these computer simulations are the following: (i) The acceleration of the soliton depends upon the dimensionless loss factor Γ and the unitless normalized bias γ. (ii) There are some cases where coupled solitons are in stable states. (iii) The creation of pairs of solitons following the transmitting soliton for $u \approx u_0$ is brought about. (iv) The velocity of the soliton given by the equation having the third differential term can exceed the limiting velocity u_0 given by the equation without the third differential term; moreover the soliton with $u/u_0 > 1.0$ is stable. (v) There are various states after collision, depending upon Γ, γ, the number of solitons, and the intervals between the solitons with same screw senses.

The propagation states of solitons which propagate along the two-dimensional transmission lines of various shapes have also been studied. To understand the behavior of solitons in two-dimensional lines, a mechanical analog of the two-dimensional SGE is shown schematically.

ACKNOWLEDGMENTS

The authors are grateful to Dr. Y. Sawada, Dr. T. Anayama, and Dr. Y. Ebina for helpful discussions.

[1]B.D. Josephson, Adv. Phys. **14**, 419 (1965).
[2]A.C. Scott, Solid-State Electron. **7**, 137 (1964).
[3]A.C. Scott, Am. J. Phys. **37**, 52 (1969).
[4]A.C. Scott, *Active and Nonlinear Wave-Propagation in Electronics* (Wiley-Interscience, New York, 1970).
[5]A.C. Scott, Nuovo Cimento B **69**, 241 (1970).
[6]A. Barone, F. Esposito, C.J. Magee, and A.C. Scott, Riv. Nuovo Cimento **1**, 227 (1971).
[7]J. Rubinstein, J. Math. Phys. **11**, 258 (1970).
[8]J.K. Perring and T.H.R. Skyrme, Nucl. Phys. **31**, 550 (1962).
[9]U. Enz, Phys. Rev. **131**, 1392 (1963).
[10]G.L. Lamb, Rev. Mod. Phys. **43**, 99 (1971).
[11]R. Hirota, J. Phys. Soc. Jpn. **33**, 1459 (1972).
[12]R. Hirota, J. Phys. Soc. Jpn. **35**, 1566 (1973).
[13]A.C. Scott, F.Y.F. Chu, and D.W. McLaughlin, Proc. IEEE **61**, 1443 (1973).
[14]T.A. Fulton, R.C. Dynes, and P.W. Anderson, Proc. IEEE **61**, 28 (1973).
[15]W.J. Johnson, Ph.D. thesis (University of Wisconsin, 1968) (unpublished).
[16]K. Nakajima, T. Yamashita, and Y. Onodera, J. Appl. Phys. **45**, 3141 (1974).